ISSN 1674-1056
http://cpb.iphy.ac.cn
http://iopscience.iop.org/cpb
中国物理 B
Chinese Physics
中国物理
Chinese Physics B

Traffic flow velocity disturbance characteristics and control strategy at the bottleneck of expressway

Jun-Wei Zeng(曾俊伟), Yong-Sheng Qian(钱勇生), Xu-Ting Wei(魏谞婷), Xiao Feng(冯骁)

Citation: Chin. Phys. B . 2018, 27(12): 124502. **doi:** 10.1088/1674-1056/27/12/124502
Journal homepage: http://cpb.iphy.ac.cn; http://iopscience.iop.org/cpb

What follows is a list of articles you may be interested in

Coordinated chaos control of urban expressway based on synchronization of complex networks

Ming-bao Pang(庞明宝), Yu-man Huang(黄玉满)
Chin. Phys. B . 2018, 27(11): 118902. **doi:** 10.1088/1674-1056/27/11/118902

Model and application of bidirectional pedestrian flows at signalized crosswalks

Tao Zhang(张涛), Gang Ren(任刚), Zhi-Gang Yu(俞志钢), Yang Yang(杨阳)
Chin. Phys. B . 2018, 27(7): 078901. **doi:** 10.1088/1674-1056/27/7/078901

Effects of rainy weather on traffic accidents of a freeway using cellular automata model

Ming-Bao Pang(庞明宝), Bo-Ning Ren(任泊宁)
Chin. Phys. B . 2017, 26(10): 108901. **doi:** 10.1088/1674-1056/26/10/108901

A new cellular automata model of traffic flow with negative exponential weighted look-ahead potential

Xiao Ma(马骁), Wei-Fan Zheng(郑伟范), Bao-Shan Jiang(江宝山), Ji-Ye Zhang(张继业)
Chin. Phys. B . 2016, 25(10): 108902. **doi:** 10.1088/1674-1056/25/10/108902

On the modeling of synchronized flow in cellular automaton models

Jin Cheng-Jie, Wang Wei, Jiang Rui
Chin. Phys. B . 2014, 23(2): 024501. **doi:** 10.1088/1674-1056/23/2/024501

Traffic flow velocity disturbance characteristics and control strategy at the bottleneck of expressway*

Jun-Wei Zeng(曾俊伟)[1], Yong-Sheng Qian(钱勇生)[1,†], Xu-Ting Wei(魏谞婷)[1], and Xiao Feng(冯骁)[2]

[1] *School of Traffic and Transportation, Lanzhou Jiaotong University, Lanzhou* 730070, *China*
[2] *School of Traffic and Transportation, Beijing Jiaotong University, Beijing* 100044, *China*

(Received 28 August 2018; revised manuscript received 10 October 2018; published online 25 November 2018)

In the three-phase traffic flow studies, the traffic flow characteristic at the bottleneck section is a hot spot in the academic field. The controversy about the characteristics of the synchronized flow at bottleneck is also the main contradiction between the three-phase traffic flow theory and the traditional traffic flow theory. Under the framework of three-phase traffic flow theory, this paper takes the on-ramp as an example to discuss the traffic flow characteristics at the bottleneck section. In particular, this paper mainly conducts the micro-analysis to the effect of lane change under the two lane conditions, as well as the effect of the on-ramp on the main line traffic flow. It is found that when the main road flow is low, the greater the on-ramp inflow rate, the higher the average speed of the whole road section. As the probability of vehicles entering from the on-ramp increases, the flow and the average speed of the main road are gradually stabilized, and then the on-ramp inflow vehicles no longer have a significant impact on the traffic flow. In addition, this paper focuses on the velocity disturbance generated at the on-ramp, and proposes the corresponding on-ramp control strategy based on it, and the simulation verified that the control strategy can reasonably control the traffic flow by the on-ramp, which can meet the control strategy requirements to some extent.

Keywords: three-phase traffic flow theory, lane change, velocity disturbance, traffic control strategy

PACS: 45.70.Vn, 89.40.Bb, 89.20.–a **DOI:** 10.1088/1674-1056/27/12/124502

1. Introduction

Since the 1950 s, the traffic flow research has achieved a lot of remarkable fruits, and a great number of models have emerged. Generally speaking, these traffic flow simulation models can be divided into two categories, *i.e.*, macroscopic and microscopic.[1–3] In the macroscopic models, Lighthill and Whithamn firstly proposed the conception of continuum model in 1955,[4] which introduces a continuum model of fluid mechanics based on the conservation law of the number of vehicles in the traffic flow, and later scholars used the solution of this model to explain the formation of traffic density waves and shock waves. Besides this, Payne introduced the kinetic equation based on the basic idea of car-following model and established a high-order traffic flow model.[5] Later, by replacing the density gradient with the velocity gradient, Jiang *et al.* proposed a new high order continuum model, and solved the unreasonable characteristic speeds in the existing models.[6,7] The micro-traffic flow model mainly studies the evolutionary characteristics of the whole traffic flow from the perspective of the interaction between vehicles, which is more in line with the essence of the traffic flow, and the representatives are car-following models and cellular automaton models. The car-following model is essentially a particle dynamics system, which postulates that vehicles need to keep a certain following distance to avoid collision, and the behavior of the following car depends on the stimulation from the front car, so as to establish the relationship between the front and the rear vehicles. Early car-following models were proposed by Reuschel[8] and Pipes.[9] On this basis, many advanced models were proposed, such as the Newell model,[10] the optimized velocity model,[11] the full velocity difference model,[12] models that consider the effect of multiple vehicles,[13] models that use different control equations under different traffic phases,[14] *etc*. However, in the car-following model, overtaking is not allowed, which is different from the real situation, and this is the main drawback of the following model. The earliest applications of cellular automata models in traffic flow originated from Cremer and Ludwig's research.[15] After Nagel and Schreckenberg proposed the NaSch model,[16] later scholars proposed a number of improved models. In 2002, Kerner proposed the KKW model, in which the vehicle speed at the next moment is determined by two steps: speed adaptation and random noise, and the influence range of the front vehicle on the following vehicle is also considered.[17]

At the end of the 20th century, the traditional traffic flow fundamental approach theory gradually lost its dominance due to its own limitations, and the three-phase traffic flow theory began to draw more and more attention. In 2004, Kerner pub-

*Project supported by the National Natural Science Foundation of China (Grant No. 51468034), the Colleges and Universities Fundamental Scientific Research Expenses Project of Gansu Province, China (Grant No. 214148), the Natural Science Foundation of Gansu Province, China (Grant No. 1606RJZA017), and the Universities Scientific Research Project of Gansu Provincial Educational Department, China (Grant No. 2015A-051).

†Corresponding author. E-mail: qianyongsheng@mail.lzjtu.cn

© 2018 Chinese Physical Society and IOP Publishing Ltd

lished the book "the Physics of Traffic",[18] representing that the three-phase flow theory has formed a complete theoretical framework. In the theory, the congested phase in the fundamental approach theory is further subdivided into synchronized phase and wide moving jams phase, which together with the free-flow phase constitutes a complete description of the states of the traffic flow in the three-phase traffic flow theory. In the congested phase, there are many congestion patterns at road bottlenecks, and the driver's preference and choice for the gap under synchronized flow will affect the congestion pattern.[19] Meanwhile, scholars believe that the synchronized flow can be stable, vehicles can maintain a state that tends to speed synchronization, and this state can lead to phase transition to either the free flow phase or the wide moving jams phase due to the perturbations in the actual traffic flow.[20] By analyzing the empirical data, Kerner *et al.* found that all the spontaneous phase transitions between different phases of the traffic flow are first order, and the traffic breakdown from free flow to the synchronized flow as well as the phase transition from the synchronized flow to the wide moving jams state only occurs randomly after the traffic density reaches a certain critical value, and its time and place are uncertain.[21] When the traffic flow is in wide moving jams, there will be a complex microscopic spatiotemporal structure appearing at the downstream jam fronts. This jam structure consists of alternations of regions in which traffic flow is interrupted and flow states of low speeds associated with "moving blanks" within the jam.[22,23] Besides these research, other analyses based on the real traffic data have revealed that the distribution of vehicles' gap is not totally chaotic. With the running of the traffic, the distribution of gap can be fitted by a concave curve. And the corresponding models are also proposed by these researchers.

At present, with the economic and social development and the expansion of the road infrastructure, single lane becomes very rare and multi-lanes are the mainstream of the roads. One important difference between single lane and two-lane road is the lane-changing behavior. In addition, there are a large number of traffic bottlenecks such as the road reduction and on-ramps that exist in real traffic, which are important causes of traffic congestion, and lane change is also involved between different lanes essentially. Therefore, it is imperative to study the lane-changing behavior of vehicles and their complicated impacts.

The core of two-lane traffic flow research is to establish a realistic lane change model to study the influence of lane-changing disturbance on road traffic flow, and in this aspect, scholars have made some meaningful attempts.[24–26] Typically, Rickert *et al.* proposed a set of lane-changing rules in 1996,[27] and later, Chowdhury *et al.* presented a symmetric two-lane CA model (abbreviated as STNS model) in 1997.[28] A similar lane change model to that in STNS was adopted by the famous simulation software TRANSIMS (short for transportation analysis and simulation system).[29,30] And Jia *et al.* improved the existing problems in STNS model and proposed H-STNS and A-STNS models.[31,32]

In the current studies, the traffic flow characteristics of the bottleneck sections have become the focus of research in the field of three-phase traffic flow. In Ref. [33], Kerner *et al.* analyzed the characteristics of traffic flow at the bottleneck section and explained the reasons of the phase transition from free flow to synchronized flow as well as the fixed disturbances at the bottleneck from micro-perspective. In Ref. [34], the authors also conducted a microscopic analysis of the generation and evolution of the velocity disturbance in the uniform section of a single road. Based on the research results in Refs. [33] and [34], this paper makes an analysis to the propagation characteristics of velocity disturbance at the bottleneck, and further its practical application is preliminarily explored in order to make use of this characteristic to put forward the corresponding on-ramp control strategy, so as to verify the theoretical research on the characteristics of the evolution of the velocity disturbance.

2. Model description and velocity disturbance analysis

The basic model is introduced in the appendix in this paper, which is a one-lane cellular automaton model under the framework of three-phase traffic flow theory. The basic model used in this paper has been introduced in Ref. [34] in detail, so we then directly conduct the study under two-lane condition.

2.1. The lane change rule and discussions

2.1.1. The lane change rule of STNS model

In the STNS model, each time step is divided into two sub-time steps; in the first sub-time step, the vehicles switch to other lane with the lane change rule; in the second time step, vehicles update according to the rules in the single lane condition. And further, the lane change rule is divided into two parts: lane-changing motivation and safety condition, namely,

(I) Lane-changing motivation

$$d_i < \min(v_i + 1, v_{\max}) \quad \text{and} \quad d_{i,\text{other}} > d_i, \tag{1}$$

(II) Safety condition

$$d_{i,\text{back}} > d_{\text{safe}}, \tag{2}$$

where v_i is the speed of the vehicle i, $v_{\max}$ is the maximum speed, $d_{i,\text{other}}$ denotes the gap in front of the i-th vehicle in other lane, $d_{i,\text{back}}$ is the gap behind the i-th vehicle in the other lane, and d_{safe} is the safe distance to avoid collision of the vehicle with the following vehicle in other lane. On the basis of a series of models,[27–32] we present our lane change rule as follows.

2.1.2. The new lane change rule

In this paper, the symmetric lane-changing rule is taken in the first sub-time step of lane change rule, and then in the second sub-time step, vehicles update in accordance with the rules in single lane model described in Ref. [34]. Here, the symmetric lane change means that the conditions for vehicles changing lanes from lane 2 to lane 1 are the same as that in the reverse process (assuming that the lanes from the left to the right are respectively lane 1 and lane 2 in the direction of the vehicle driving). Specifically,

(i) Lane-changing motivation

$$\text{lane } 1 \leftrightarrow \text{lane } 2: \ v_i \geq d_i, \quad \text{or} \quad d_{i,\text{other}} > d_i, \tag{3}$$

(ii) Safety condition.

Based on the above analysis, we conclude that drivers with different drive preferences always have significantly different driving strategies, so we further subdivide the drivers into two categories, *i.e.*, aggressive and conservative. The aggressive driver's safety distance is taken as the maximum distance traveled by an aggressive driver during a single update time step, while the conservative driver's safety distance is taken as the maximum distance that a conservative driver can travel within a single update time step. So we set the following safe distance conditions:

$$d_{\text{safe}} = \begin{cases} V_{\text{max,ag}} & \text{if driver is aggressive,} \\ V_{\text{max,co}} & \text{if driver is conservative,} \end{cases} \tag{4}$$

$$\text{lane } 1 \leftrightarrow \text{lane } 2: \ d_{\text{safe}} > d_{i,\text{back}}, \tag{5}$$

where $v_{\text{max,og}}$ and $v_{\text{max,co}}$ are respectively the maximum speeds of aggressive drivers and conservative drivers. Meanwhile, in order to prevent the "ping-pong effect" that appears inconsistent with the actual traffic in the simulation, this paper also sets the lane-changing probability p_{change} to avoid it; when the above conditions are met in the simulation, a random number is generated, and if the random number is less than p_{change}, lane change is conducted.

2.2. Simulation results and analysis

Simulations are carried out on a circular road with the periodic boundary condition. In the simulations, every cell denotes 1.5 m. Each vehicle occupies 5 cells, and the length of the road is 2000 cells. Considering the research in Ref. [33] that most drivers tend to choose a safer speed, the proportion of aggressive vehicles is set as 15%. The parameters of vehicle performances and models are listed in Table 1 and Table 2 below.

Table 1. The parameters of vehicle.

Vehicle type	Maximum speed		Acceleration		Deceleration	
	Within D/(cells/s)	Outside D/(cells/s)	Within D/(cells/s^2)	Outside D/(cells/s^2)	Within D/(cells/s^2)	Outside D/(cells/s^2)
Aggressive	17	20	3	4	3	4
Conservative	13	17	2	3	2	3

Table 2. The parameters of models.

p_{macc}	p_{m}	p_{ss}	p_{sm}	k_{s}	D_0	τ	t_{c}
0.65	0.15	0.6	0.2	3	0	1 s	5 s

The survey takes 20 independent simulations, and every simulation runs 6000 time steps. Among those simulations, the first 3000 time steps are discarded to avoid the influence of the initial state on the results. And the final result is the average of these simulations.

2.2.1. The fundamental diagram

We conduct the simulation under periodic boundary conditions, and set p_{change} as 0.6. The fundamental diagram is shown below. In Fig. 1(a), as the traffic density increases, the flow rate basically linearly increases before the density reaches the critical value k_{a}, after which it no longer grows rapidly and reaches the maximum, and then the flow is gradually reduced until it drops to 0 due to the number of vehicles on the road at the time is too large. In Fig. 1(b), it can be seen that the vehicle speed can maintain a steady maximum until the traffic density reaches k_{a}, after which the speed gradually decreases as the interaction between vehicles on the road increases. Furthermore, compared to the fundamental diagram in Ref. [34], we can find that the critical density k_{a} in Fig. 1 of this paper is larger than that in Fig. 1 of Ref. [33], which is due to the fact that under the two-lane condition, the road resources can be fully utilized; therefore, the flow has a greater value

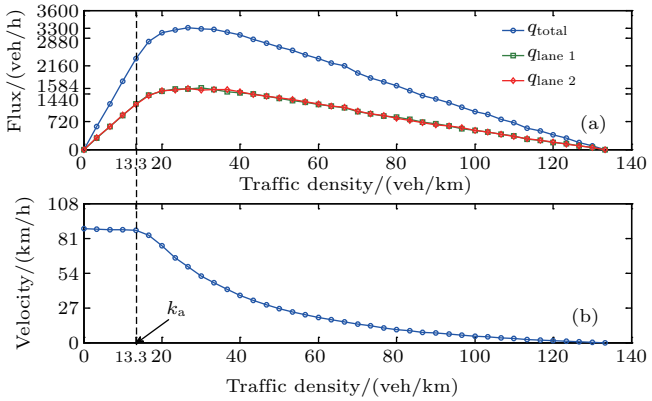


Fig. 1. (color online) Fundamental diagram. (a) The averaged flow–density diagram. (b) The averaged velocity–density diagram.

before reaching the critical state. In addition, it can be seen from Fig. 1(a) in Ref. [34] that the flow has a small drop after reaching the maximum, and then decreases more gently; but in this Fig. 1(a), the flow curve keeps a smooth decline when the flow reaches the maximum. Similarly, this is because vehicles can make full use of the road resources by changing lanes when the road flow reaches the maximum, namely, as the traffic density increases, the vehicles on the road can effectively utilize the gap between vehicles, so that the traffic flow does not drop sharply.

2.2.2. The lane change effect analysis

In the above sections, we have analyzed the basic model of two-lane traffic flow. In this section, we discuss the effect of lane change behavior; in general, it has a significant impact on the road traffic flow. For the current lane, if the traffic density is large, changing these vehicles to other lane will reduce the local traffic pressure in this lane and induce a local dissipation acceleration wave. For the target lane, if the traffic density of the lane is in the critical state near the phase transition, these vehicles entering through changing the lane will induce a local diffusion deceleration wave, prompting the occurrence of the phase transition. This is the dual role of lane change.

The simulation in this section is carried out under open boundary conditions and p_{in} is used to denote the probability of the vehicles entering from the main road. We simulate the traffic flow on uniform road sections under different p_{in} to investigate the microscopic role of the lane changing.

As can be seen from Fig. 2, when $p_{\text{in}} = 0.3$, the trajectory curves of vehicles are relatively smooth and the slopes are basically the same, indicating the traffic flow is in the free flow state.

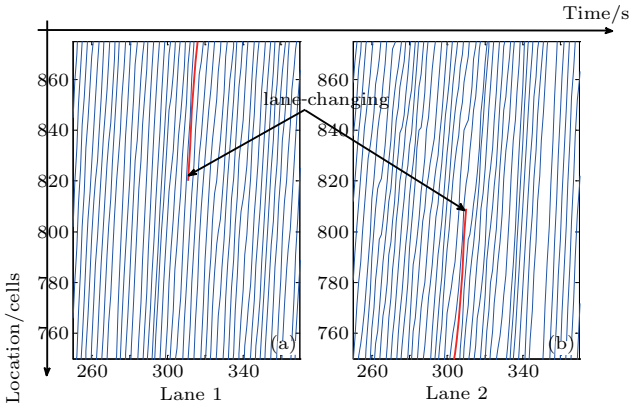


Fig. 2. (color online) Vehicle travel trajectories ($p_{\text{in}} = 0.3$).

In Fig. 2, for convenience reading, the vehicle that changes lane is marked in red. Either in lane 1 shown in Fig. 2(a) or in lane 2 shown in Fig. 2(b), the vehicle that changes lane does not have a significant impact on the traffic flow, and the following vehicles in the two lanes still remain in the previous driving states and their speeds are not affected by the lane change of the front car.

Hence, it can be concluded that in the free flow, vehicle lane change behavior does not have a significant impact on the traffic flow.

Figure 3 shows the vehicle travel trajectory when $p_{\text{in}} = 0.5$. It can be seen that some trajectories are tortuous and the slopes of curves are somewhat different, indicating that the traffic flow is in the light synchronized flow phase between free flow and synchronized flow.

In Fig. 3(a), the velocity of the following vehicles has no obvious changes. In other words, the lane-changing vehicles have almost no effect on lane 1. However, for lane 2, most of the vehicles' driving curves are relatively even and smooth before the lane change vehicles enter. There is no obvious mutual influence and velocity disturbance that can propagate between vehicles. However, after vehicles switch lanes, the following vehicle decelerates immediately to keep safety, and this deceleration induces a velocity disturbance, and its following vehicles also make a similar deceleration behavior. That is, these lane change vehicles induce a velocity disturbance of backward propagation after entering lane 2, resulting in a local deceleration wave and local congestion. Thus, when the traffic density on the road reaches a certain critical value, the lane change behavior of the vehicle will cause the vehicles on the other lane to decelerate continuously and induce a velocity disturbance of backward propagation, and this disturbance will cause local congestion. This simulation result is also in line with the reality.

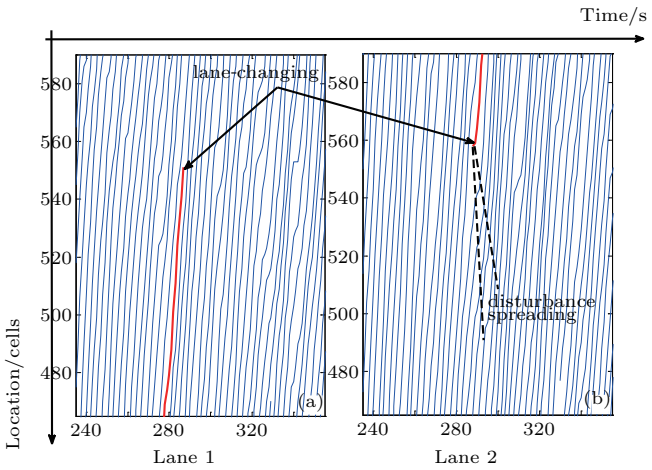


Fig. 3. (color online) Vehicle travel trajectories ($p_{\text{in}} = 0.5$).

It can be seen from Fig. 4 that almost all vehicle's trajectories and their slopes have large differences and are unevenly distributed, so that it can be considered that the traffic flow is already in the synchronized flow phase at this time.

In Fig. 4(a), the traffic density of lane 1 is relatively large, and there is a velocity disturbance appeared propagating from the downstream to the upstream of the road before vehicles change lanes. This velocity disturbance severely restricts the driving of following vehicles, so there are two vehicles in Fig. 4(a) that change lanes when conditions are met, which

weakens the effect of velocity disturbance. It can be seen that before the first lane-changing vehicle is swapped out of lane 1, its following vehicles need to adjust their speed to adapt the speed changes of the front car. However, after it drives away from lane 1, these following vehicles can maintain a stable driving speed due to the enough road gap caused by the exit of the preceding vehicle, namely, the velocity disturbance propagated to the upstream is weakened due to the lane change behavior of the vehicle. For the second lane-changing vehicle, similarly, its following vehicles are also affected before it switches into another lane. However, the speed adjustment range and frequency of the following vehicles are significantly smaller than those of the first lane-changing vehicle. After the vehicle is swapped out of lane 1, the following cars are no longer affected by the velocity disturbance propagated from the upstream and thus the disturbance is completely dissipated because of the lane-changing behavior of the vehicle.

Therefore, we can conclude that when the traffic flow of a lane is in the synchronized flow phase and the vehicle density in a local section of the adjacent lane is low, the lane change behavior of vehicles can weaken or even block the propagation of the velocity disturbance on the road and reduce the traffic density of the local road section, resulting in a local acceleration wave, and prompting the local synchronous flow to the free-flow phase transition.

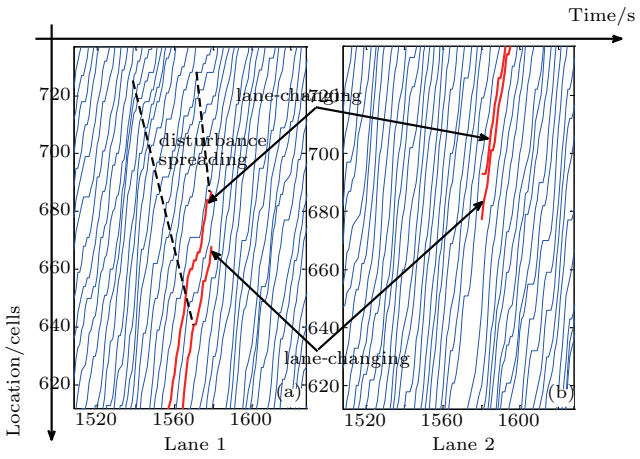


Fig. 4. (color online) Vehicle travel trajectories ($p_{\text{in}} = 0.7$).

3. The on-ramp control strategy

In the above sections, we introduce a symmetric lane change rule to extend the single lane model into two lane CA model and analyze the impact of the lane change on the traffic flow under two-lane conditions.

For the current on-ramp control strategies of expressway, whether they are timed control schemes or adaptive sensing control strategies is mostly based on traffic statistics on main roads and on-ramps of expressways. Indeed, the flow rate can reflect the operation states of traffic flow. However, when the traffic flow is in the synchronized flow phase, the flow rate and speed are no longer linear one-to-one correspondence. Therefore, making on-ramp control solely based on the detected traffic data is likely to result in a "control blind area" in the synchronized flow phase. When the traffic flow is in heavy synchronized flow phase, if the flow rate of main road is not significantly reduced, it is hard to generate the phase transition from the synchronized flow to the free flow only by adjusting the inflow rate of the on-ramp, thus missing the best adjustment time of the on-ramp. Therefore, on the basis of the previous improved two-lane model, we attempt to analyze the velocity characteristics of the traffic flow at the upstream and downstream of the on-ramp from the microscopic angle, and further put forward the corresponding on-ramp control strategy of expressway.

3.1. Basic settings and hypotheses

The numerical simulation in this section is based on an expressway model with an on-ramp, and the simulated road section is shown in Fig. 5 below. The basic model parameters are the same as the previous section.

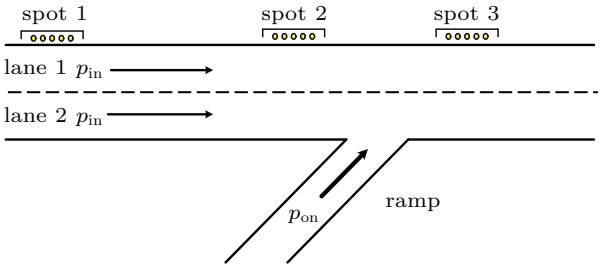


Fig. 5. The schematic diagram of the on-ramp system.

The open boundary condition is adopted in this study, and p_{in} and p_{on} denote the probabilities of the vehicles entering from the two main lanes and the on-ramp, respectively; the on-ramp is located at the 1200th–1220th cells on lane 2.

The rules for the on-ramp are as follow: searching the ramp road section continuously until find a space gap which can accommodate a vehicle, then generate a car with probability p_{on}, and its type be allocated according to the mixed probability 15%.

3.1.1. Flow rate and speed analysis

In this section, we record the flow rate and velocity under the different p_{in} and p_{on}. The simulation parameters in this section are the same as above except for the open boundary.

As can be seen from Fig. 6, with the increase of p_{in}, the flux of the road first increases, and then fluctuates around it after reaching a certain value. While p_{in} is low, with the increase of p_{on}, the flux under the same p_{in} shows a significant increase. The reason is that when p_{in} is low, the number of vehicles entering from the main road is small; as p_{on} increases, a large number of vehicles enter the road from the ramp, making up for the insufficient flow of the main road.

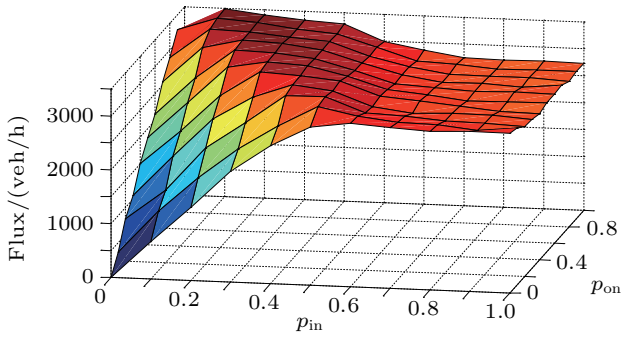


Fig. 6. (color online) The flux under different p_{in} and p_{on}.

Figure 7 shows the average velocity under different p_{in} and p_{on}. When p_{in} and p_{on} are low, the velocity is relatively large. As p_{in} and p_{on} increase, the number of vehicles on the road increases correspondingly, then the interaction between them becomes stronger and stronger, and the velocity gradually decreases. When p_{in} is low, with the increase of p_{on}, most of the vehicles enter the main road from the ramp, and there are fewer vehicles at the upstream of the on-ramp and will not be affected by those vehicles before they reach the on-ramp; However, when p_{in} is large and p_{on} is low, most of the vehicles are entering from the main road, and they mostly pass through the on-ramp and will be affected by the vehicles entering from the on-ramp to reduce the speed. As a result, the speed at the p_{in} end close to 0 in Fig. 7 is greater than the speed at the p_{on} end in the vicinity of 0. And when both p_{in} and p_{on} are close to 1, the velocity reaches the minimum.

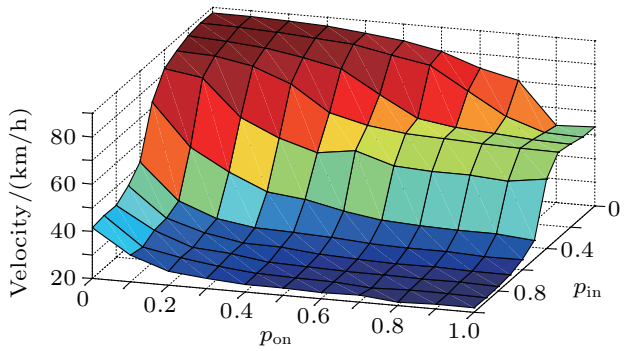


Fig. 7. (color online) Average velocity under different p_{in} and p_{on}.

In order to further analyze the impact of p_{in} and p_{on} on the traffic flow phases, we respectively select the flux and velocity curves when is 0.3, 0.6, and 0.9 for analysis.

Figure 8 is the flow velocity curve with the growth of p_{in} when p_{on} is 0.3, 0.6, and 0.9. As can be seen from Fig. 8(a), when p_{in} is zero, the flow rate curve gradually increases with the growth of p_{on}. As mentioned above, this is due to the fact that as p_{in} is fixed and small, the number of vehicles entering from the on-ramp increases with the growth of p_{on}, thereby also resulting in the smaller velocity in Fig. 8(b). As the increase of p_{in} reaches the critical value k_a, the velocity curves under the conditions of $p_{on} = 0.6$ and 0.9 are very close. After p_{in} exceeds the critical value, the two velocity curves decrease in a substantially parallel manner; and at this critical value, the flow curves corresponding to different p_{on} in Fig. 8(a) also start to coincide. In this case, there are already more vehicles on the road. Vehicles entering the main road from the ramp at this time will have a greater impact on the following cars, causing a large number of vehicles on the main road to queue up. When the vehicles entering the ramp turn off the ramp, the vehicles queuing on the main road pass the ramp more densely and the vehicles on the ramp cannot enter the main road. So, increasing p_{on} in this case can not significantly affect the traffic flow and speed of the main road. Therefore, the corresponding flow and speed curves no longer have obvious differences or even start to gradually coincide. With further increase of p_{in}, the flux and velocity curves at $p_{on} = 0.3$ also show similar trends when p_{on} values are 0.6 and 0.9. Finally when p_{in} reaches k_c, the ramp entry probability p_{on} will no longer affect the traffic flow of the main road, and the traffic flow tends to be the same value; although the traffic flow rate when p_{on} is 0.3 is still steadily higher than the other two cases, there is no longer an obvious difference, and the velocity curves at $p_{on} = 0.6$ and 0.9 start to overlap.

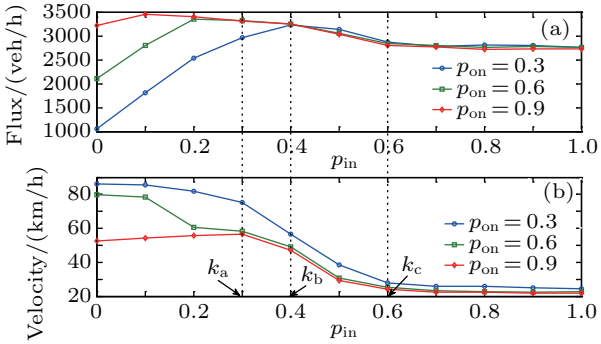


Fig. 8. (color online) Average flux and velocity under different p_{on}.

3.1.2. Velocity disturbance analysis

In order to better understand the impact of vehicles entering from the ramp on the traffic flow, this section analyzes the traffic flow under fixed p_{in} and different p_{on} conditions from a micro perspective, and the traffic flow characteristics under different p_{on} are compared.

Firstly, we analyze the situation when $p_{in} = 0.3$ and $p_{on} = 0.2$. Figure 9 shows the trajectories of the vehicles in lane 2, in which the green lines and blue lines respectively denote the vehicles entering from the ramp and the main road.

Figure 10, from left to right, top to bottom, shows the corresponding speed of vehicles which are marked in bold in Fig. 9 when passing through different spots.

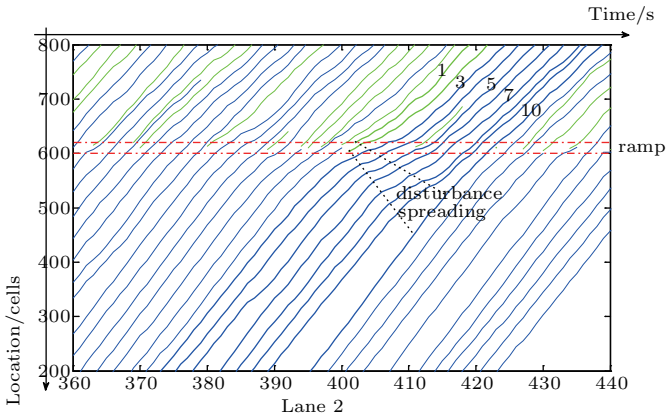


Fig. 9. (color online) Vehicle trajectories on lane 2.

It can be seen from Figs. 9 and 10 that when the vehicle 1 and the vehicle 2 enter the main road from the ramp, the following vehicle 3 decelerates to adapt the preceding vehicle (Fig. 10(c)), and this deceleration makes it continue to maintain a low speed as it passes the 583th to 628th cells. Meanwhile, the following vehicle 4 also decelerates due to the deceleration of the vehicle 3, and also maintains the low speed when passing through the 581th to 624th cells. Thus it can be seen that after entering lane 2, the vehicle 1 and vehicle 2 induce a velocity disturbance propagating upstream. However, the low driving speed of vehicle 3 during disturbance period produces a large gap from the preceding vehicle. Therefore, after leaving the influence range of vehicle 2, the vehicle 3 can continuously accelerate, resulting in a speed peak as shown in Fig. 10(c). Similar to the propagation of velocity disturbance, this local acceleration also leads to a continuous acceleration of the following vehicle, and thus induces a local acceleration wave.

It can be seen from Fig. 10 that the local acceleration wave and velocity disturbance have the same propagation direction, that is, propagating upstream of the ramp, but the effect is opposite. The upstream spread velocity disturbance causes the following vehicles to decelerate, while the local acceleration wave induced by the speed peak makes the low speed vehicles accelerate to exit this congestion group. Hence, when the disturbance occurs for a period of time, the vehicle downstream of the ramp can maintain a high velocity, and the deceleration disturbance will gradually propagates upstream, causing the speed of the vehicles at the upstream of the ramp decreases. And this is also in line with the definition of synchronized flow in the three-phase traffic flow theory.

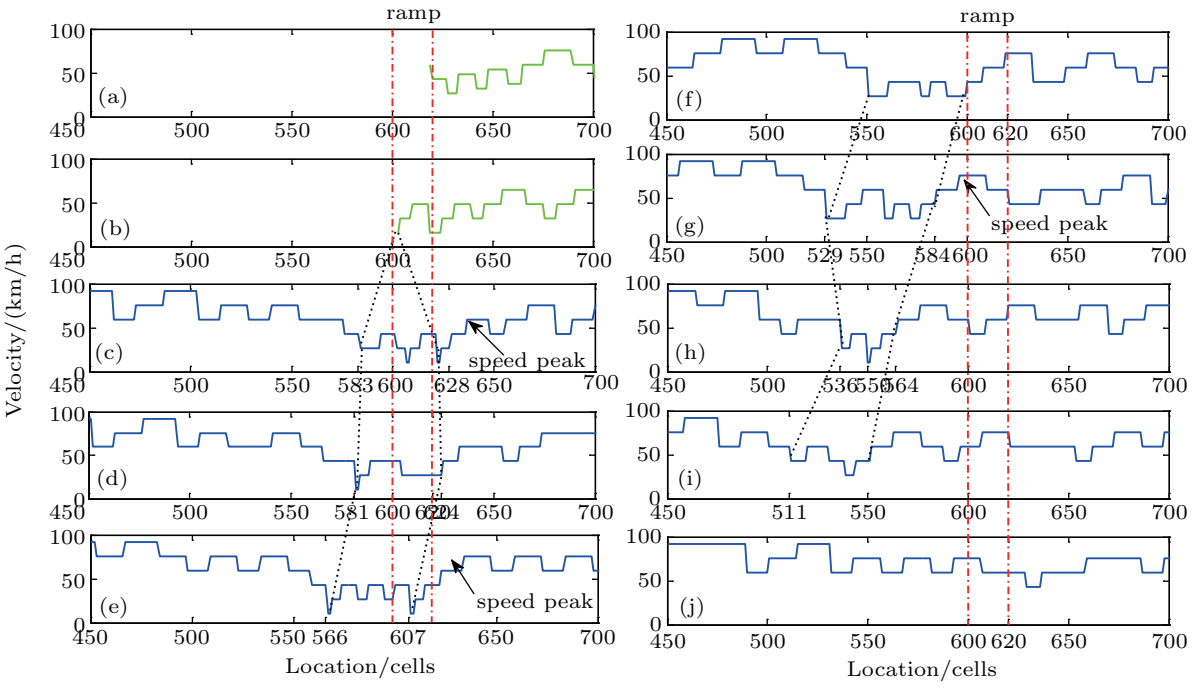


Fig. 10. (color online) Individual vehicle speed along vehicle trajectories marked in Fig. 9.

Figure 11 shows the speed of the vehicle 3, vehicle 5, and vehicle 7, which are marked in Fig. 9. It can be seen from the figure that the vehicle 3 is firstly affected by the velocity disturbance, making it decrease the speed to the synchronized flow, and the following vehicles 5 and 7 also decelerate to adapt to the preceding vehicle. The velocity disturbance gradually propagates upstream with the synchronized flow until it dissipates (at lower vehicle densities) or continues to propagate upstream (at higher densities). However, after the disturbance dissipates, the vehicle accelerates and produces a speed peak. The speed

of the vehicle returns to the free-flow speed and the local free flow phase propagates upstream along with the velocity peak. Therefore, it can be concluded that velocity disturbance and speed peaks are two competing roles that have the same propagation direction but opposite effects. When the propagation velocity of the velocity disturbance is faster than the speed peak, the local synchronized flow accelerates to spread upstream. Otherwise, the synchronized flow will gradually dissipate in the process of upstream propagation.

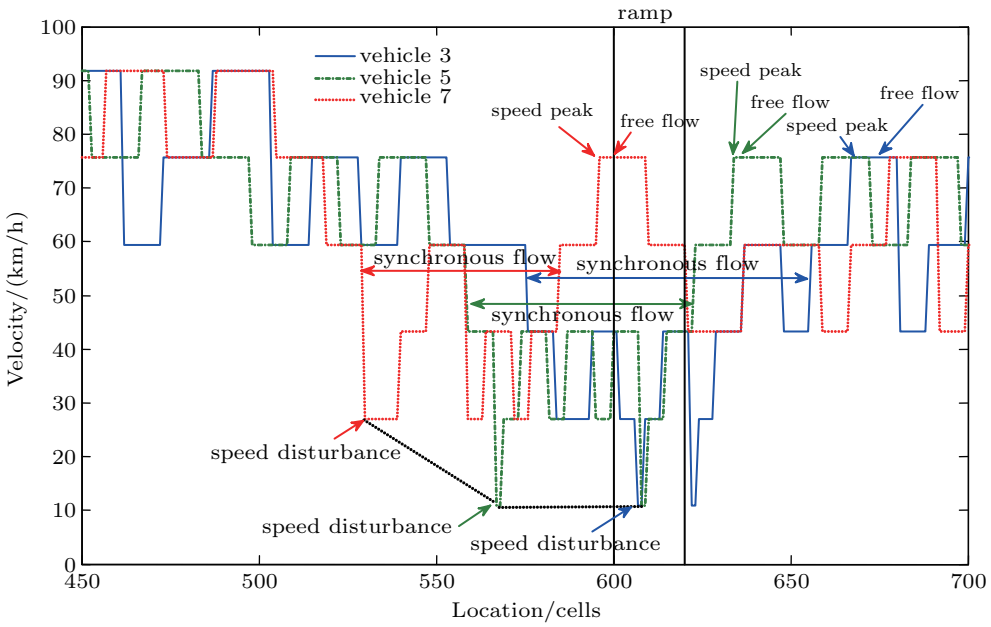


Fig. 11. (color online) Individual vehicle speed along vehicle trajectories marked in Fig. 9.

3.2. The on-ramp control strategy

In this section, we mainly analyze and compare the speed of vehicles at different spots on the expressway, and establish on-ramp control strategies based on different speed characteristics.

3.2.1. The characteristics of speed change

Figures 12 and 13 show the local traffic flow and average speed at the selected spots. Three spots are selected in the simulation, each of which contains 5 virtual detectors, and the average of the data obtained from the five virtual detectors in each spot is taken as the data we use. The first virtual detector in the first spot (Figs. 12(a) and 13(a)) is located at the 20th cell, and thereafter the remaining virtual detectors are placed every 5 cells. The first virtual detector of the second spot (Figs. 12(b) and 13(b)) is placed at 5 cells in front of the ramp and the remaining four virtual detectors are located every 5 cells in the anti-flow direction. The third spot (Figs. 12(c) and 13(c)) is located at 5 cells behind the ramp, and the rest virtual detectors are set every 5 cells in the direction of the traffic flow. Figures 12(d) and 13(d) show the total traffic flow statistics and the average speed of the entire section, respectively.

As can be seen from Fig. 12, in the case of p_{on} is large and the flux tends to be stable, if p_{on} is also large, the local flow at spot 1 is greater than spot 2, and the flow at spot 3 is the highest. It can be seen that when p_{in} and p_{on} are large, the vehicles entering from the on-ramp have a more obvious impact on the upstream main road traffic flow, whereas the initial road section of the road is less affected as it is far away of the ramp, so the flow rate is higher.

It can be seen from Fig. 13 that the observed velocity change at spot 1 is not affected by the probability p_{on} in most cases. However, in the case of $p_{in} < 0.5$, the average speed of the entire road section at the observation point 2 and spot 3, which are respectively at the upstream and downstream of the ramp, is more sensitive to the probability p_{on}.

Comparing Figs. 12 and 13, it can be seen that the velocities measured at different spots are more sensitive to p_{on} than the flux.

In order to further analyze the difference of velocity between different observation points, we separately use the data obtained when and values are 0.3, 0.6, and 0.9, respectively, and compare the velocity curves under different combinations of them.

Figure 14 shows the velocity under different p_{on} with the increase of p_{in}. When $p_{in} < 0.4$, in all cases of Figs. 14(a), 14(b), and 14(c), the spot 1 of the main road has the highest speed, followed by the spot 2 on the upstream of the ramp, and then the spot 3 on the downstream of the ramp is the lowest. While p_{in} is between 0.4 and 0.7, the velocity measured

at the spot 3 begins to exceed that of spot 2. We believe this is because as p_{in} increases, the velocity disturbances occurring at the ramp propagate more to the upstream, and at the same time the propagation speed of the velocity peak toward upstream is lower than the speed of the velocity disturbance propagating upstream. Therefore, the impact of upstream local synchronized flow of the ramp on the traffic flow gradually becomes greater. As p_{in} continues to increase, when it exceeds 0.7, the local velocity downstream of the ramp even exceeds the velocity at the upstream spot 1, so it can be considered that the traffic flow upstream of the ramp has been basically in the synchronized flow phase.

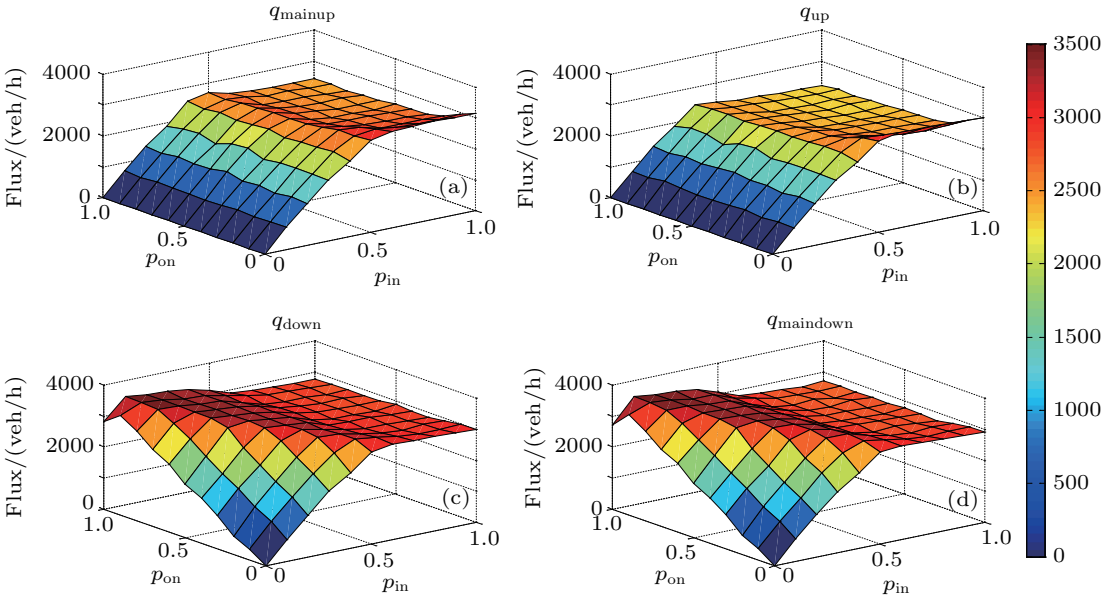


Fig. 12. (color online) Flux at different spots.

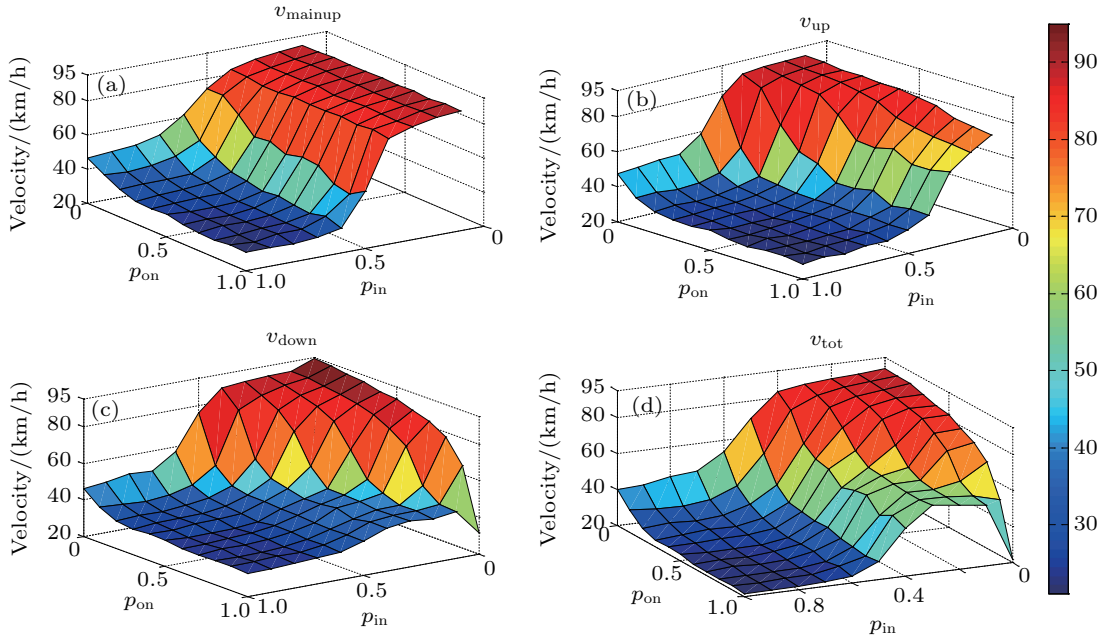


Fig. 13. (color online) Velocity at different spots.

Figure 15 shows the velocity with the increase of p_{on} under different p_{in}. When p_{in} is low ($p_{\text{in}} = 0.3$), the spot 1 has the highest speed, the spot 2 is the second, and the spot 3 is the lowest. This result is similar to that in Fig. 14 when p_{in} is less than 0.4. We believe that the velocity disturbance caused by the ramp does not affect the traffic flow at this moment, and the speed that the velocity disturbance propagates to the upstream is lower than that of the speed peak to the upstream. As p_{in} increases ($p_{\text{in}} = 0.6$), the measured velocity at spot 3 is higher than that of spot 2, which is also same as the situation when p_{in} is between 0.4 and 0.7 in Fig. 14. We believe that the velocity disturbance caused by the ramp in this state al-

ready has a certain impact on the traffic flow of the main road, and some vehicles are greatly restricted and cannot maintain a high driving speed. As the p_{in} further increases, the velocity at the downstream spot 3 has exceeded the velocity at the upstream spot 1, indicating that there has been a synchronized flow spread to the entrance of the main road; in this case, it is very difficult to dissipate the velocity disturbance on the road section simply by adjusting the on-ramp inflow rate. When p_{in} reaches 0.9, as long as there are few vehicles entering the main road from the ramp, it will cause the velocity disturbance which is difficult to dissipate completely ($p_{on} > 0.1$). In this state, the observed velocity at the downstream spot 3 is completely higher than the velocity obtained at the two upstream spots, and it is very difficult to improve the traffic flow on the main road solely by adjusting the p_{on}, so completely shutting down the ramp in this state is the only option.

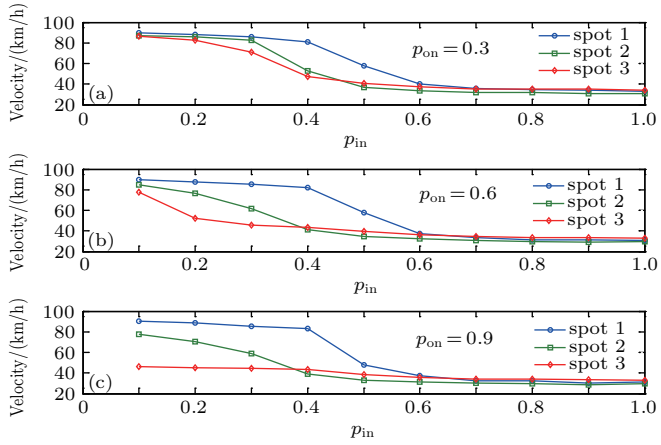


Fig. 14. (color online) Average velocity under different p_{on}.

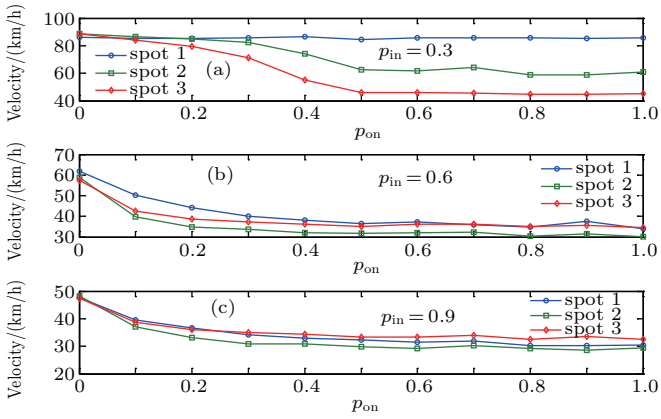


Fig. 15. (color online) Average velocity under differen p_{in}.

3.2.2. The on-ramp control strategy

From the analysis of the above section, we find that under different combinations of p_{on} and p_{in}, the speeds measured at different spots on the road section are different. When the total traffic flow in the road section is in free flow, the local velocity disturbance generated at the ramp cannot obviously affect the global operation status of the traffic flow, and the disturbance will dissipate very quickly. When the on-ramp inflow rate increases, the local velocity disturbance generated at the ramp will gradually spread to the upstream of the main road. If the vehicles entering from the on-ramp are further increased, they will have a greater impact on the overall traffic operation states of the road section, and the velocity disturbance generated at the ramp will propagate upstream from the ramp along with the synchronized flow until it reaches the initial section of the road.

In the above three stages, we find that in the first stage, the relationship between the velocity measured at the three observation spots on the road section can be kept as the maximum value at spot 1, followed by the spot 2, and lowest at spot 3. In the second stage, the spot 1 can still maintain the maximum speed, while the measured speed at spot 2 is lower than spot 3. And in the last stage, the speed at the spot 3 has exceeded the speed measured by the spot 1. We believe that long-term control of traffic flow in free flow phase with a high average speed cannot make full use of expressway resources, which is a waste of infrastructure resources. However, controlling the traffic flow in the heavy synchronized flow phase with very low average speed is very likely to cause global congestion induced by velocity disturbance, which essentially loses the meaning of on-ramp control. Therefore, the reasonable control state range should be to control the traffic flow in light synchronized flow phase upstream of the ramp, in which the vehicles entering from the ramp will still induce velocity disturbances, but the resulting local synchronized flow does not fully propagate to the whole road section upstream of the ramp, and the traffic flow and average speed still maintain at a high level. This state is just corresponding to the case that the speed at spot 1 is the highest, and the speed measured at spot 3 is higher than that of spot 2.

Hence, we take this state as the target control state of the control strategy. In this control strategy, we adjust p_{on} to balance the traffic flux between upstream and downstream, which is reflected by the velocity of traffic flow. Based on the location of the virtual detectors, the scenarios can be divided into 4 kinds. For the first scenario, the local velocity of spot 3 is lower than the value at spot 2 and spot 1, which means that there are few vehicles on the main road. Therefore, more vehicles can drive into the highway. For the second scenario, the velocity at the spot 1 is lower than the velocity at the spot 3, and the velocity at the spot 3 is lower than the value at the spot 2. In this scenario, the disturbance begins to appear, but the influence made by the disturbance is small. For this reason, more vehicles can still drive in the main road. For the third scenario, the velocity at the spot 1 is the lowest, and the velocity at the spot 3 is lower than the value at the spot 2. In this scenario, the disturbance begins to propagate upstream and make a great

influence on the main road. In this scenario, the number of vehicles should be reduced to promote the dissipation. For the last scenario, the velocities at different spots are stable, and the adjustment of p_{on} is not necessary.

Based on the above analysis, the control strategy is proposed and the pseudo-code is as follow. In the pseudo-code, the vdigmain, vdigup, and vdigdown are the velocities at the spot 2, spot 1, and spot 3, respectively. The pon is the p_{on}.

```
function[pon]=control(vdigmain,vdigup,vdigdown,pon)
if vdigdown<vdigup && vdigup<vdigmain
    pon=min(pon+0.2,1);
elseif vdigup<vdigdown && vdigdown<vdigmain
    pon=min(pon+0.1,1);
elseif vdigup<vdigmain && vdigmain<vdigdown
    pon=max(pon-0.2,0);
else
    pon=pon;
End
```

To test the effectiveness of the control strategy, we continuously measure the traffic flow for one hour under different p_{in}. Figure 16 shows the average speed per minute observed under different p_{in} and the corresponding p_{on}. It can be seen from Figs. 16(a), 16(b), and 16(c) that under this control strategy, the speed at spot 3 is higher than the speed at spot 2. In Fig. 16(a), we can see that there are fewer vehicles on the road at this time, the vehicles can maintain a steady speed driving state within the measure period, and the speed at spot 3 is higher than that of spot 2 under this ramp control strategy for a long period of time. In Fig. 16(d), p_{on} is relatively large, that is, the on-ramp mostly keeps completely open to make up for the lack of the main road traffic flow due to the lower p_{in}. Compared to the opposite simulation data at $p_{in} = 0.3$ in Fig. 14, it can be seen that this control strategy is effective when the traffic density is low. As can been seen from Fig. 16(b), the measured velocity at spot 3 is still higher than the velocity at spot 2, but they have no obvious trend to the spot 1. In Fig. 16(e), we can find that whenever there is an upward trend in the velocity of the spot 3, p_{on} will decrease to properly control and adjust the velocity disturbance caused by the ramp. Compared to the case of $p_{in} = 0.6$ in Fig. 14, by this control strategy adjustments, the p_{on} within one hour is mostly lower than 0.6; although there are cases that the speeds measured at spot 1 are lower than spot 3, it can still be adjusted to return to the target control state.

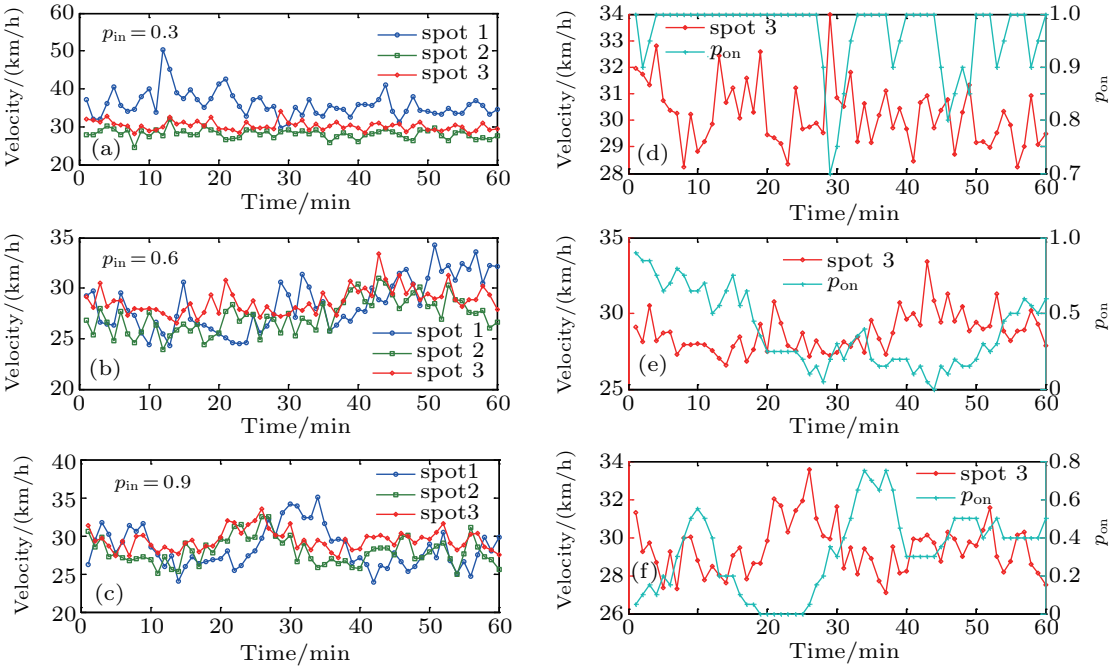


Fig. 16. (color online) Velocity at different spots and under different p_{in}.

Comparing to the case of $p_{in} = 0.9$ in Fig. 14, we can see that in the absence of the control strategy, no matter how much p_{on} is, there will be a case that the speed at spot 1 will be lower than the velocity at spot 3. However, it can be seen in Fig. 16 that under the regulation of p_{on}, although the above case still exists, the control strategy has not completely failed, and it can still adjust the traffic flow states to a certain extent.

4. Conclusions

In this study, it is found that due to the lane change rules, the road resources can be more fully utilized under the two-lane condition. Correspondingly, the critical traffic density of the traffic flow is larger, and the curve of the traffic flow declines more smoothly after reaching the maximum. In addition, when the traffic flow is in the free flow phase, the lane

change behavior of vehicles has no obvious effect on the traffic flow. However, when traffic density is large, the lane-changing behavior will weaken or cause the propagation of velocity disturbance in traffic flow. Even if both the current lane and target lane are in free flow phase before changing lanes, after the vehicles switch into the other lane, they will cause velocity disturbances which will affect the traffic flow states of the swap-in lane. In the case that the traffic density further increases, if there is a velocity disturbance in the swap-out lane, continuous vehicle lane changes will gradually weaken the propagation process of the velocity disturbance to the upstream, resulting in the phase transition from local synchronized to the free-flow in the current lane.

Based on the velocity disturbance characteristics of two-lane traffic flow, this paper uses a modified two lane CA model to simulate the ramp sections of expressway and compares the vehicle speed at different observation spots and under different conditions; on this basis, a ramp control strategy is proposed. In the process of simulating this strategy, we find that when the traffic flow is low, this strategy can effectively adjust the on-ramp inflow rate to make up for the shortage of the main road traffic flow. When the flow is high, the strategy can control the number of vehicles entering the main road from the ramp timely, so that the overall traffic flow can be gradually adjusted back to the target state if it is out of the control of the target state. Especially, when the traffic flow exceeds the adjustment range, the strategy can still play a regulatory role, so that it is unnecessary to completely shut down the on-ramp.

Appendix A

The basic model is proposed in Ref. [34], and we introduce this model in the appendix. This model can reproduce some typical phenomena which can be explained by the three-phase traffic flow theory. The relevant proof and discussion can be found in Ref. [34].

Step 1 Speed adaptation

The speed adaptation mechanism can be found in the KKW model described above in this paper. In Eq. (A1), $v_{i,\max,n}$ is the maximum velocity of the vehicle i corresponding to v_{free} in the KKW model, and d_i corresponds to $v_{s,n}$ which denotes the distance between the vehicle i and the preceding vehicle $i-1$. The speed of the vehicle i at the next moment should be less than $v_{i,\max n}$ to avoid collision. $v_{i,\text{des}}$ corresponds to $v_{c,n}$, and D corresponds to D_n which is the synchronization distance between vehicles. If the vehicle is within the previous car's synchronization distance, the vehicle adjusts its velocity to adapt to the previous vehicle based on the velocity difference between the two vehicles. The initial velocity of the vehicle can be calculated by

$$\tilde{v}_{i,n+1} = \max[0, \min(v_{\text{i,max}\,n}, v_{i,\text{des}}, d_i)], \tag{A1}$$

where $v_{i,\text{des}}$ is defined by

$$v_{i,\text{des}} = \begin{cases} v_{i,n} + acc_i \cdot \tau, & \text{if} \quad d_i > D, \\ v_{i,n} + \text{sign}(v_{i-1,n} - v_{i,n}) \cdot acc_i \cdot \tau, & \text{if} \quad d_i \le D. \end{cases} \tag{A2}$$

where $\text{sign}(x)$ is a sign function; when $x > 0$, $\text{sign}(x) = 1$; when $x = 0$, $\text{sign}(x) = 0$; and when $x < 0$, $\text{sign}(x) = -1$. This formulation describes the case that when the vehicle i is out of the preceding vehicle $i-1$, the vehicle i is accelerated with a fixed acceleration. And there are three cases when the vehicle i enters the synchronization distance of the preceding car: case 1, $v_i < v_{i-1}$, then the vehicle i accelerates to chase the previous vehicle; case 2, $v_i = v_{i-1}$, the vehicle remains the current driving state; case 3, $v_i > v_{i-1}$, vehicle i decelerates.

The vehicle accelerates and decelerates to adjust its own velocity or to indicate the random condition in driving in the speed adaptation and velocity fluctuation. In this paper, the deceleration is essentially different from that of the brake to avoid a collision, which is revealed by using d_i to constrain in formula. This assumption is identical to the KKW model. Therefore, as to simplify the model, the acceleration and deceleration rates are the same in speed adaptation.

This paper employs the linear function to calculate the synchronization distance D

$$D = D_0 + k_s \cdot v_{i,n} \cdot \tau, \tag{A3}$$

where D_0 and k_s are positive constants.

The above steps of speed adaptation are identical to KKW model. In addition, the drivers are divided into two types, *i.e.*, the aggressive one and the conservative one, in the speed adaptation phase.

According to practical experience, the aggressive drivers tend to drive at a higher speed and maintain a smaller distance with the former vehicle, while the conservative drivers tend to do the opposite. Thus, the aggressive driver employs greater acceleration for chasing the former vehicle in time. Consequently, the aggressive drivers decelerate excessively to avoid the collision when the preceding vehicle decelerates due to its own higher moving velocity.

Regardless of the fact that whether the driver is aggressive or conservative, when the vehicle is far away from the preceding car, its velocity and acceleration are higher because the driver does not worry about the collision with the former vehicle. The smaller the gap between the two vehicles is, the lower the velocity and the acceleration are.

For describing the diversity of driving behavior, the maximum speed and acceleration of the vehicle are subdivided according to the type of a driver and the distance from the vehicle ahead. The subscripts *agg* and *con* denote variables of aggressive and conservative drivers, respectively. Consequently, $v_{\text{max agg,in}}$ and $acc_{\text{agg,in}}$, as well as $v_{\text{max con,in}}$ and $acc_{\text{con,in}}$, are

the maximum moving velocity and acceleration corresponding to the aggressive and conservative vehicles, respectively, when the vehicles keep within the synchronization distance of the former vehicle. Similarly, $v_{\max\,\mathrm{agg,out}}$ and $acc_{\mathrm{agg,out}}$, as well as $v_{\max\,\mathrm{con,out}}$ and $acc_{\mathrm{con,out}}$, respectively represent the maximum moving velocity and acceleration corresponding to the aggressive and conservative vehicle when the vehicle stays outside the synchronization distance of the former vehicle.

Hence, the refined maximum speed $v_{\max n}$ and the acceleration acc are as follows:

$$v_{i,\max,n}=\begin{cases} v_{\max\,\mathrm{agg.in}} & \text{if} \quad d_i \le D \quad \text{and driver is aggressive,} \\ v_{\max\,\mathrm{agg.out}} & \text{if} \quad d_i > D \quad \text{and driver is aggressive,} \\ v_{\max\,\mathrm{con.in}} & \text{if} \quad d_i \le D \quad \text{and driver is conservative,} \\ v_{\max\,\mathrm{con.out}} & \text{if} \quad d_i > D \quad \text{and driver is conservative,} \end{cases} \tag{A4}$$

$$acc_i=\begin{cases} acc_{\mathrm{agg.in}} & \text{if} \quad d_i \le D \quad \text{and driver is aggressive,} \\ acc_{\mathrm{agg.out}} & \text{if} \quad d_i > D \quad \text{and driver is aggressive,} \\ acc_{\mathrm{con.in}} & \text{if} \quad d_i \le D \quad \text{and driver is conservative,} \\ acc_{\mathrm{con.out}} & \text{if} \quad d_i > D \quad \text{and driver is conservative.} \end{cases} \tag{A5}$$

Step 2 Fluctuation of speed

When the driver keeps a particular driving state for a long time, the sensitivity to outside stimuli will decrease. In this paper, the velocity changes of the former vehicle are regarded as the external stimulation to the following vehicle, so the speed difference between vehicles should be taken into consideration. The reduction of the sensitivity causes the driver to maintain the driving state at the last moment; thereby, the response delay appears. Specifically, due to the loss of the sensitivity, regardless of the road conditions, the probability of the start delay of vehicles which stand still for a long time is higher than the vehicles which have just stopped. For the same reason, a driver of a vehicle that has been in movement for a long time (the speed of the vehicle is higher or lower than the preceding vehicle, *i.e.*, acceleration or deceleration with respect to the preceding vehicle) tends to maintain the previous driving state, whether closer to or far away from the vehicle ahead. However, for the vehicle driving with a short duration, the driver's sensitivity from external stimulus is higher, so the driver can respond to the speed change of the preceding vehicle in time and generate random speed changes (such as avoiding the obstacles, *etc.*). The tendency of this response delay is defined as the speed adjustment based on the probability in the paper.

The above-mentioned speed fluctuation caused by the response delay is generated in the course of the vehicle adaptation to the speed change of the front vehicle; thus, it appears to be based on the initial velocity from the speed adaptation in the last step. This phenomenon can be described as

$$v_{i,n+1}=\begin{cases} \max[0,\min(\tilde{v}_{i,n+1}+dec_i\cdot\mathrm{sign}(v_{i-1,n}-v_{i,n})\cdot d_i)] & \text{if} \quad t_{i,n,s}>t_c \ \ \& \ \ v_{i,n}\neq 0 \ \ \& \ \ \mathrm{rand}()<p_{\mathrm{macc}}, \\ \max(0,\tilde{v}_{i,n+1}-dec_i\cdot\tau) & \text{if} \quad t_{i,n,s}\le t_c \ \ \& \ \ v_{i,n}\neq 0 \ \ \& \ \ \mathrm{rand}()<p_{\mathrm{m}}, \\ \max(0,\tilde{v}_{i,n+1}-dec_i\cdot\tau) & \text{if} \quad t_{i,n,s}>t_c \ \ \& \ \ v_{i,n}=0 \ \ \& \ \ \mathrm{rand}()<p_{\mathrm{ss}}, \\ \max(0,\tilde{v}_{i,n+1}-dec_i\cdot\tau) & \text{if} \quad t_{i,n,s}\le t_c \ \ \& \ \ v_{i,n}=0 \ \ \& \ \ \mathrm{rand}()<p_{\mathrm{sm}}, \end{cases} \tag{A6}$$

where t_{c} is the critical time for drivers to lose the sensitivity of the stimulus, $t_{i,n,s}$ is the time of vehicle i keeping a certain driving state, p_{macc} and p_{ss} are the probabilities of reaction delay for the moving and stopping states that have reduced the drivers' sensitivity, and p_{m} and p_{sm} are the randomization probabilities of speed change in the moving and stopping states, respectively, for the driver's sensitivity is still high.

The velocity fluctuation in this paper describes such a velocity change behavior: for the vehicle with reduced sensitivity and still moving, the reaction delay occurs with a probability p_{macc}, which can make the vehicle be closer to or far away from the front vehicle depending on the speed difference between the two vehicles, usually leading to the driver's over-acceleration or over-deceleration behavior. This mechanism/setting can exacerbate the over-acceleration and over-deceleration behavior of the vehicles within the synchronized distance and promote the phase change.

This model takes the same value for the speed variations acc_i and dec_i in the speed adaptation and speed fluctuation process. Thus, for vehicles that have stopped, if their sensitivity has reduced, a greater randomization probability p_{ss} is given to indicate their tendency to remain the current state (*i.e.*, parking). Meanwhile, for drivers with higher sensitivity, a lower randomization probability p_{sm} is taken to describe vehicles which can start in time. Furthermore, a lower randomization probability p_{m} is used to reflect the random variation

of speed for the vehicles that have higher sensitivity without stopping.

For vehicles that the velocity is non-zero at time n, since the adjustment of their acceleration and deceleration depends on the drivers' behavior and road condition, the amplitude of their adjustment is minor. Therefore, the new model denotes the same variation of acceleration and deceleration as dec_i. This hypothesis is the same as acc_i of the speed adaptation, and the two values are the same. Different symbols are taken to mark the two speed variations in order to reflect the change caused by different reasons.

$$dec_i = \begin{cases} dec_{\text{agg.in}} & \text{if } di \le D \text{ and driver is aggressive,} \\ dec_{\text{agg.out}} & \text{if } d_i > D \text{ and driver is aggressive,} \\ dec_{\text{con.in}} & \text{if } d_i \le D \text{ and driver is conservative,} \\ dec_{\text{con.out}} & \text{if } d_i > D \text{ and driver is conservative.} \end{cases} \tag{A7}$$

Step 3 Update of the location of the vehicle

The $v_{i,n+1}$ is calculated by the two steps above at time $n+1$, and the location of vehicle is determined by

$$loc_{i,n+1} = loc_{i,n} + v_{i,n+1} \cdot \tau. \tag{A8}$$

And the parameters recording the vehicle's movement conditions are also updated

$$t_{i,n+1,s} = \begin{cases} t_{i,n,s}+1 & \text{if } v_{i,n} \neq 0 \ \& \ \text{sign}(v_{i-1,n} - v_{i,n}) = \text{sign}(v_{i-1,n+1} - v_{i,n+1}), \\ 0 & \text{if } v_{i,n} \neq 0 \ \& \ \text{sign}(v_{i-1,n} - v_{i,n}) \neq \text{sign}(v_{i-1,n+1} - v_{i,n+1}), \\ t_{i,n,s}+1 & \text{if } v_{i,n} = v_{i,n+1} = 0, \\ 0 & \text{if } v_{i,n} = 0 \ \& \ v_{i,n+1} \neq 0. \end{cases} \tag{A9}$$

References

[1] Khan Z H, Shah S A A and Gulliver T A 2018 *Chin. Phys. B* **27** 070202
[2] Wang Y and Chen Y Y 2015 *Chin. Phys. B* **24** 038902
[3] Pan W, Xue Y, Zhao R and Lu W Z 2014 *Chin. Phys. B* **23** 058902
[4] Lighthill M J and Whitham G B 1955 *Proc. Roy. Soc. London A* **229** 317
[5] Payne H J 1971 *Math. Models Publ. Sys.* **28** 51
[6] Jiang R, Wu Q S and Zhu Z J 2002 *Transp. Res. B* **36** 405
[7] Jiang R, Wu Q S and Zhu Z J 2001 *Sci. Bull.* **46** 345
[8] Reuschel A 1950 *Fahrzeugbewegungen in der KolonneBeigleichformig beschleunigtem oder vertzogerten Oesterrich Ingr Arch* **4** 193
[9] Pipes L A 1953 *J. Appl. Phys.* **24** 274
[10] Newell G F 1961 *Oper. Res.* **9** 209
[11] Bando M, Hasebe K and Nakayama A 1995 *Phys. Rev. E* **51** 1035
[12] Jiang R, Wu Q and Zhu Z 2001 *Phys. Rev. E* **64** 017101
[13] Helbing D, Hennecke A, Shvetsov V and Treiber M 2001 *Transp. Res. B* **35** 183
[14] Hennecke A, Treiber M, Helbing D 2000 *Macroscopic Simulation of Open Systems and Micro-Macro Link*. In: Helbing D, Herrmann H J, Schreckenberg M, and Wolf D E (eds.) *Traffic and Granular Flow* '99 (Berlin, Heidelberg: Springer)
[15] Cremer M and Ludwig J 1986 *Math. Comput. Simul.* **28** 297
[16] Nagel K and Schreckenberg M 1992 *J. de Physique I* **2** 2221
[17] Kerner B S, Klenov S L and Wolf D E 2002 *J. Phys. A: Math. Gen.* **35** 9971
[18] Kerner B S 2004 *The Physics of Traffic* (Heidelberg, Berlin, New York: Springer)
[19] Kerner B S 2002 *Phys. Rev. E* **65** 046138
[20] Kerner B S 2012 *Phys. Rev. E* **85** 036110
[21] Kerner B S, Rehborn H, Schäfer R P, Klenov S L, Palmer J, Lorkowski S and Witte N 2013 *Physica A-Stat. Mech. Its Appl.* **392** 221
[22] Kerner B S, Klenov S L and Hiller A 2006 *Phys. Rev. E* **73** 046107
[23] Kerner B S 2013 *Physica A-Stat. Mech. Its Appl.* **392** 5261
[24] Ke H T, Liu X H, Guo M M and Wu Z 2015 *Chin. Phys. B* **24** 098901
[25] Liu X H, Ke H T, Guo M M and Wu Z 2016 *Chin. Phys. B* **25** 048901
[26] Tian H H and Xue Y 2012 *Chin. Phys. B* **21** 070505
[27] Rickert M, Nagel K, Schreckenberg M and Latour A 1996 *Physica A-Stat. Mech. Its Appl.* **231** 534
[28] Chowdhury D, Wolf D E and Schreckenberg M 1997 *Physica A-Stat. Mech. Its Appl.* **235** 417
[29] Smith L, Beckman R, Anson D, Nagel K and Williams M 1995 Transims: transportation anslysis and simulation system, Office of Scientific & Technical Information Technical Reports
[30] Nagel K, Wolf D E, Wagner P and Simon P 1998 *Phys. Rev. E* **58** 1425
[31] Jia B, Jiang R and Wu Q S 2005 *Physica A* **348** 544
[32] Li X G, Jia B and Gao Z Y 2006 *Physica A-Stat. Mech. Its Appl.* **367** 479
[33] Kerner B S, Klenov S L, Hermanns G and Schreckenberg M 2013 *Physica A-Stat. Mech. Its Appl.* **392** 4083
[34] Qian Y S, Feng X and Zeng J W 2017 *Physica A-Stat. Mech. Its Appl.* **479** 509